

Supporting Information for:

Aqueous p-type dye-sensitized solar cells based on the tris(1,2-diaminoethane) cobalt(II)/(III) redox mediator

Wanchun Xiang^{a,b,*}, Joshua Marlow^a, Peter Bäuerle^c, Udo Bach^{d,e,f}, Leone Spiccia^{a*}

^aSchool of Chemistry, Monash University, Victoria 3800, Australia Fax: +61 3 9905 4597; Tel: +61 3 9905 4526; E-mail: Leone.Spiccia@monash.edu

^bState Key Laboratory of Silicate Materials for Architectures, Wuhan University of Technology, Hubei, 430070, China; Email: xiangwanchun@whut.edu.cn

^cInstitute for Organic Chemistry II and Advanced Materials, University of Ulm, Albert-Einstein-Allee 11, 89081 Ulm (Germany)

^dDepartment of Materials Engineering, Monash University, Victoria 3800, Australia

^eCommonwealth Scientific and Industrial Research Organization, Materials Science and Engineering, Flexible Electronics Theme, Clayton South, Victoria 3169, Australia

^fMelbourne Centre for Nanofabrication, 151 Wellington Road, Clayton, VIC 3168, Australia

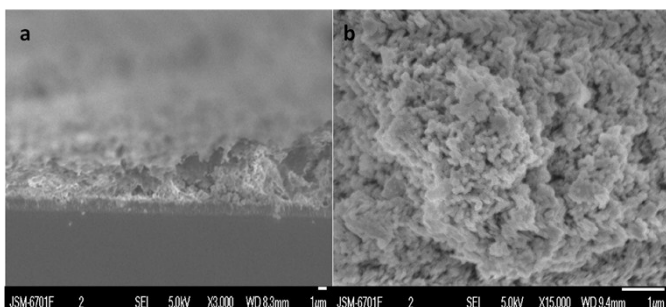


Figure S1 Scanning electron microscope of mesoporous NiO film on FTO substrate. a) Cross-sectional image, b) top-view image.

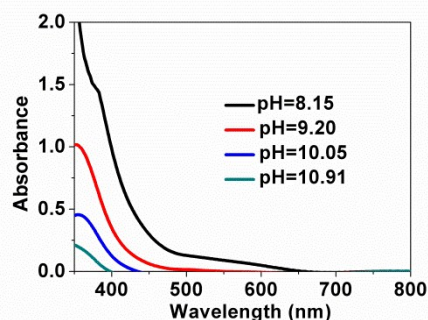


Figure S2 UV-Visible spectra of aqueous electrolytes with different pHs. The electrolytes contained 0.6 M $[\text{Co}(\text{en})_3](\text{BF}_4)_2$, 0.07 M $[\text{Co}(\text{en})_3](\text{BF}_4)_3$, 0.9 M LiBF_4 and 0.3 M NMBI in deionized water, where either boric acid or 1,2-diaminoethane were used to adjust the electrolyte pHs. An aqueous solution containing 0.9 M LiBF_4 and 0.3 M NMBI was used as blank.

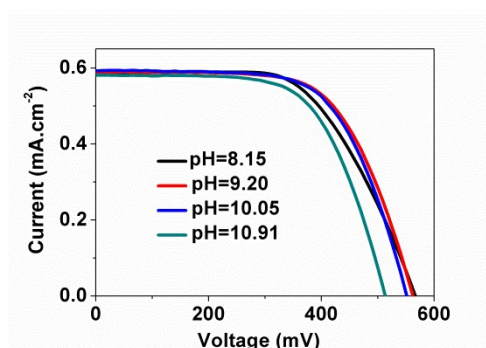


Figure S3 J-V curves for p-type DSCs based on $[\text{Co}(\text{en})_3]^{2+/3+}$ electrolytes with different pHs at 0.1 sun light intensity illumination.

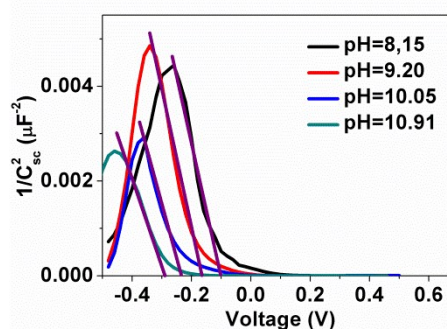


Figure S4 Mott-Schottky behavior of NiO contacting with different pH electrolytes. The experiment was carried out by a three-electrodes setup. A 7×7 mm NiO film was used for working electrode. Platinum wire and Ag/AgCl were used as counter and reference electrodes, respectively. Boric acid and 1,2-diaminoethane were used to adjust the pH of the electrolytes. The scan range was from -0.5 V to 0.5 V vs Ag/AgCl and the frequency was chosen at 1 Hz for figure plotting. The linear fitting results were extrapolated to $1/(C_{\text{sc}})^2 = 0$.

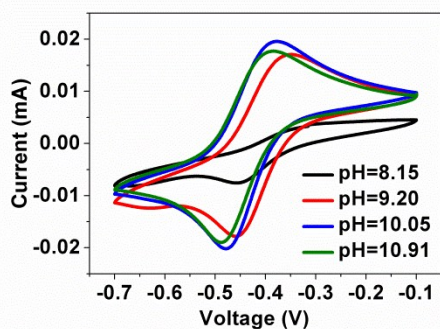


Figure S5 Cyclic voltammetry of $[\text{Co}(\text{en})_3]^{2+/3+}$ redox mediator in different pH electrolytes. The measurement was conducted at a 20 mV s^{-1} scan rate in the range of -0.7 to -0.1 V vs Ag/AgCl . The aqueous electrolyte solution contained $6 \text{ mM } [\text{Co}(\text{en})_3](\text{BF}_4)_2$, $0.7 \text{ mM } [\text{Co}(\text{en})_3](\text{BF}_4)_3$ and 0.1 M potassium chloride, in water, where boric acid and extra 1,2-diaminoethane were used to adjust electrolyte pHs.

Table S1 Optimization of $[\text{Co}(\text{en})_3](\text{BF}_4)_2$ concentration in aqueous electrolytes used in p-type DSCs at a pHs of 8.15. Other components in electrolyte are: $0.10 \text{ M } [\text{Co}(\text{en})_3](\text{BF}_4)_3$, 0.10 M NMBI, 0.50 M LiBF_4 in water. The NiO film thickness is $2.4 \mu\text{m}$. Device performance data is the average of at least three devices. Photovoltaic parameters were recorded under light intensities of 1000 mW cm^{-2} .

$[\text{Co}(\text{en})_3](\text{BF}_4)_2$ (M)	V_{OC} (mV)	J_{SC} (mAcm^{-2})	FF	η (%)
0.2	584 ± 3	3.52 ± 0.02	0.29 ± 0.01	0.60 ± 0.10
0.4	572 ± 5	3.81 ± 0.01	0.34 ± 0.01	0.73 ± 0.06
0.6	564 ± 4	4.44 ± 0.01	0.40 ± 0.01	1.01 ± 0.05
0.8	553 ± 6	4.52 ± 0.01	0.39 ± 0.01	0.97 ± 0.07

Table S2 Optimization of $[\text{Co}(\text{en})_3](\text{BF}_4)_3$ concentration in aqueous electrolytes used in p-type DSCs at a pH of 8.15. Other components in electrolyte are: $0.60 \text{ M } [\text{Co}(\text{en})_3](\text{BF}_4)_2$, 0.10 M NMBI, 0.70 M LiBF_4 in water (NiO film thickness is $2.4 \mu\text{m}$; photovoltaic parameters recorded at 1000 mW cm^{-2} ; data averaged for at least three devices).

$[\text{Co}(\text{en})_3](\text{BF}_4)_3$ (M)	V_{OC} (mV)	J_{SC} (mAcm^{-2})	FF	η (%)
0.07	582 ± 8	5.90 ± 0.04	0.41 ± 0.01	1.42 ± 0.17
0.27	600 ± 6	4.85 ± 0.02	0.41 ± 0.01	1.19 ± 0.13
0.47	615 ± 7	4.72 ± 0.05	0.42 ± 0.01	1.22 ± 0.11
0.67	595 ± 5	4.22 ± 0.02	0.45 ± 0.01	1.13 ± 0.10

Table S3 Optimization of NMBI concentration in aqueous electrolyte used in p-type DSCs at a pH of 8.15. Other components in electrolyte are: $0.2 \text{ M } [\text{Co}(\text{en})_3](\text{BF}_4)_2$, $0.10 \text{ M } [\text{Co}(\text{en})_3](\text{BF}_4)_3$, 0.30 M LiBF_4 in water (NiO film thickness is $2.4 \mu\text{m}$; photovoltaic parameters recorded at 1000 mW cm^{-2} ; data averaged for at least three devices).

NMBI (M)	V_{OC} (mV)	J_{SC} (mAcm^{-2})	FF	η (%)
0	362 ± 5	0.67 ± 0.01	0.47 ± 0.01	0.11 ± 0.03
0.1	696 ± 8	2.79 ± 0.04	0.23 ± 0.01	0.45 ± 0.09
0.3	684 ± 6	3.64 ± 0.07	0.23 ± 0.01	0.57 ± 0.17
0.5	672 ± 7	1.68 ± 0.01	0.25 ± 0.01	0.28 ± 0.07

Table S4 Optimization of LiBF_4 concentration in aqueous electrolyte for p-type DSCs at a pH of 8.15. Other components in electrolyte are: $0.60 \text{ M } [\text{Co}(\text{en})_3](\text{BF}_4)_2$, $0.10 \text{ M } [\text{Co}(\text{en})_3](\text{BF}_4)_3$, 0.30 M NMBI in water (NiO film thickness is $2.4 \mu\text{m}$; photovoltaic parameters recorded at 1000 mW cm^{-2} ; data averaged for at least three devices).

LiBF_4 (M)	V_{OC} (mV)	J_{SC} (mAcm^{-2})	FF	η (%)
0	531 ± 2	0.43 ± 0.01	0.59 ± 0.01	0.14 ± 0.02
0.5	553 ± 7	3.35 ± 0.02	0.41 ± 0.01	0.75 ± 0.16
0.7	583 ± 10	4.79 ± 0.08	0.41 ± 0.01	1.14 ± 0.20
0.9	609 ± 8	6.02 ± 0.05	0.40 ± 0.01	1.46 ± 0.17
1.2	581 ± 8	6.14 ± 0.10	0.40 ± 0.01	1.42 ± 0.13

Table S5 Optimization of NiO film thickness for aqueous p-type DSCs assembled using an electrolyte with pH of 8.15. The components in electrolyte are: $0.20 \text{ M } [\text{Co}(\text{en})_3](\text{BF}_4)_2$, $0.10 \text{ M } [\text{Co}(\text{en})_3](\text{BF}_4)_3$, 0.10 M NMBI, 0.30 M LiBF_4 in water (NiO film thickness is $2.4 \mu\text{m}$; photovoltaic parameters recorded at 1000 mW cm^{-2} ; data averaged for at least three devices).

Thickness (μm)	V_{OC} (mV)	J_{SC} (mAcm^{-2})	FF	η (%)
0.8	692 ± 10	2.81 ± 0.05	0.25 ± 0.01	0.49 ± 0.20
1.6	689 ± 8	4.13 ± 0.07	0.27 ± 0.01	0.77 ± 0.19
2.4	682 ± 7	4.30 ± 0.05	0.30 ± 0.01	0.89 ± 0.17
3.2	661 ± 6	4.22 ± 0.04	0.29 ± 0.01	0.80 ± 0.10
4.0	651 ± 7	4.12 ± 0.04	0.24 ± 0.01	0.65 ± 0.11

Table S6 Valence band potentials (E_{VB}) and acceptor-state densities (N_A) of NiO in contact with different pH electrolytes. Data were fitted and calculated from Mott-Schottky curves in **Figure S4** using equation (1) given in main text.

pH	E_{VB} (V vs NHE) extrapolated	$N_A(\times 10^{19}\text{cm}^{-3})$
8.15	0.30±0.04	2.23±0.06
9.20	0.24±0.02	2.05±0.13
10.05	0.17±0.06	1.91±0.08
10.91	0.11±0.04	1.82±0.04

Table S7 Parameters obtained by CV measurements for the redox mediators with different pH electrolytes (vs NHE).

pH	E_{Ox} (V)	E_{Red} (V)	E_{Mid} (V)	$\Delta E (= E_{Ox} - E_{Red})$ (V)	I_{Ox}/I_{Red}
8.15	- 0.14±0.04	-0.25±0.03	-0.19±0.06	0.12±0.03	0.44±0.03
9.20	- 0.16±0.06	-0.26±0.03	-0.21±0.05	0.10±0.05	1.03±0.06
10.05	- 0.19±0.03	-0.27±0.02	-0.23±0.03	0.08±0.02	0.99±0.02
10.91	- 0.19±0.03	-0.28±0.04	-0.24±0.04	0.09±0.03	0.97±0.04

